VIII. TUNNELEXPERIMENT

Ivar Giaever(1960) utförde tunnelexperiment med en av tunnelelektroderna i form av en supraledare. Resultaten blev en av de vackraste verifikationerna av den mikroskopiska supraledningsmodellen. Energigap och tillståndstäthet för excitationer ur grundtillståndet kunde bestämmas. Finstruktur ger fononspektra och elektron-fonon-kopplingens styrka. Många fler effekter kan studeras som anisotropier, Fermihastighet, ordningsparameter, parbrytning, gaplöshet, bundna tillstånd och multipartikeltunneling. Foton- och fonon-assisterad tunneling ger detektormöjligheter. Fotoner och fononer kan också genereras. Josephsoneffekterna, som berör tunneling av elektronpar, ger många rika tillfällen till grundläggande studier av fysik såväl som applikationer. Vi ägnar ett helt kapitel (XII) åt Josephsoneffekterna.

Våra studier av supraledande tunneleffekter (kvasipartikeltunneling) underlättas av

(i) artikeln av Meservey och Schwartz: "Equilibrium Properties", kapitel III - "Density of States by Tunneling Measurements" (ingår i boken utgiven av Parks);

(ii) Schrieffers artikel "Single Particle Tunneling in Superconductors" (ingår i Burstein-Lundqvist: "Tunneling Phenomena in Solids");

(iii) "The Microscopic Theory of Superconductivity - Verifications and Experiments" av Claeson och Lundqvist.

Andra gångbara referenser är "Tunneling Phenomena in Solids (E. Burstein & S. Lundqvist, eds, Plenum, 1969); L. Solymar, "Superconductive Tunneling and Applications" (Chapman & Hall, 1972).

VIII.1 Grundläggande ekvationer

Repetera tunneleffekt behandlad i kvantfysikkurs. Se Meservey och Schwartz resp Schrieffer.

VIII.2 Supraledande tunneling

Se samma artiklar för supraledande tillståndstäthet och specifika effekter orsakade av supraledning. Experimentell procedur berörs i M-S samt behandlas vid laboration.

VIII.3 Temperaturberoende energigap och $2\Delta(0)/kT_c$.

Se C-L. Notera att $\Delta(T)$ relativt temperaturoberoende för $T<0.5T_c$ och den snabba nedgången nära T_c. $2\Delta(0)/kT_c > 3.53$ förklaras av teori för stark koppling.

VIII.4 Anisotropier

Vi har approximerat elektron-fonon-växelverkan med en isotrop storhet V, vilken också gav ett isotropt energigap. Men egentligen beror elektron-fonon-kopplingens styrka på riktningarna hos elektronerna före och efter spridningen, $V_{kk'}$. Således bör även energigapet bli riktningsberoende. Se C-L för detaljer.

Här har vi även förklaringen till att T_c vanligtvis går ned då små mängder föroreningar löses i ett rent grundämne. (Vid fortsatt legering kan T_c fortsätta nedgången eller istället öka, vilket främst beror på hur elektronstrukturen påverkas - initialverkan är en minskning.) I en ren metall med anisotrop växelverkan fås olika gap i olika riktningar. T_c motsvarar det högsta värdet på energigapet (i den riktningen fås kortslutning då T_c underskrides). Med föroreningar fås ett genomsnittligt, isotropt, gap, som naturligtvis är mindre än det maximala värdet. Således fås en minskning av T_c.

Egentligen borde vi kanske vara förvånade att den mikroskopiska teorin gäller även för orena metaller. Låt oss säga, att fria medelvägglängden $\approx$ 100 Å. Då blir spridningstiden $\tau \approx 10^{-14}$s och osäkerhetsrelationen ger $\Delta E \approx \hbar/\tau \approx 1000\ k_B$, dvs motsvarar temperaturen 1000 K. Energibreddningen är således avsevärt större än såväl gap- som Debyeenergin, de två viktiga storheterna i den supraledande växelverkan. Använde vi oss av planvågsfunktioner, som vi gjort tidigare, finner vi att energiosäkerheten helt skulle skyla de subtila effekter, som ger supra-

ledning. Anderson visade att om man istället använder sig av vågfunktioner, som redan inbegriper spridning, och kombinerar tidsreverserade sådana till elektronparfunktioner, så kan en BCS-liknande formalism användas. Men nu med en isotrop växelverkan V istället för $V_{kk'}$.

Övergången från ren till förorenad supraledare bör bestämmas av $\Delta E \gtrsim \hbar/\tau \gtrsim 2\Delta$. Eftersom BCS-värdet för koherenslängden, $\xi = \hbar v_F/\pi\Delta(0)$ ser vi att anisotropier bör försvinna då $\ell = v_F\tau$ är av storleksordningen ξ. Detta stämmer rätt väl med den experimentellt bestämda region inom vilken T_c påverkas av ℓ .

VIII.5. Tomasch-effekt

Effekten, som beskrivs i C-L, illustrerar vackert hur excitationer ur det supraledande tillståndet har såväl elektron- som hålkaraktär.

VIII.6. Foton- och fononstimulerad tunneling

Belyses en supraledande tunnelövergång med fotoner, vars frekvens understiger gapfrekvensen, $h\nu<2\Delta$, kan man se struktur i I-V-kurvan - strömbidrag vid gapspänningen minus multiplar av fotonenergin. Effekten, som även uppträder för fononer, diskuteras i C-L.

En mycket viktig tillämpning är en blandarmottagare för höga frekvenser baserad på S-I-S (eller ev S-I-N) övergångar - en s k kvasipartikelblandare. Konduktansbidragen, pga den fotonstimulerade tunnelprocessen, ger korskopplingstermer (signal - lokaloscillator) som bidrager till hög konverteringsgrad, rentav tillförstärkning, om energibreddningen av I-V-kurvan vid energigapet är mindre än fotonenergin. Den höga konversionen innebär att blandarelementets låga brustemperatur kan nyttjas optimalt i en känslig mottagare för t ex radioastronomi. Vi återkommer till denna högfrekvenstillämpning senare.

VIII.7. Multipartikeltunneleffekten

Vi har diskuterat tunneling av enskilda elektroner, eller s k kvasipartiklar. Man kan även tänka sig att två enskilda elektroner tunnlar samtidigt mellan två supraledare, vilket skulle ge upphov till en singularitet vid $2\Delta/2$ jämte den vanliga gapsingulariteten. Liknande för n elektroner, struktur vid $2\Delta/n$. Sannolikheten för samtidig tunneling måste dock bli mycket låg. Om man för enskilda elektroner har en tunnelsannolikhet proportionell mot tunnelmatrisen i kvadrat, T^2, så skulle man få T^4 för två-partikeltunneling etc. För att få en avsevärd effekt får man anta att man har svaga områden i tunnelbarriären, vars yta är relativt liten så att bidraget till en-elektrontunnlingen ej blir så dominerande som det till fler-elektrontunnlingen. Se f ö C-L för behandling.

Två elektroner kan även tunnla korrelerade, som ett elektronpar. Josephson visade att sannolikheten för en sådan tunnelprocess är proportionell mot T^2 och ej mot T^4. Den blir således i högsta grad betydande, och vi återkommer med en detaljerad diskussion senare.

VIII.8. Fononeffekter. Stark koppling hos supraledare.

Redan i de första tunnelmätningarna på aluminium-bly-övergångar fanns det struktur i ström-spänningskurvorna vid spänningar över gapspänningen. Strukturerna blur mycket mera framträdande om man betraktar derivatorna dI/dV eller d^2I/dV^2 mot V (laborationen visar detta). Skillnaderna i energi mellan de extra strukturerna och gapenergin motsvarar karakteristiska fononfrekvenser i metallen ifråga.

Och det är ju ej förvånande att man kan spåra fononeffekter i supraledande tunneleffekter. Elektron-fonon-kopplingen är ju avgörande för supraledning och då den är stark blir fononstrukturen i tunnelkurvorna väl märkbar.

Tunnelspektroskopin har utvecklats till en utomordentlig teknik.att kvantitativt kartlägga fononspektrat och elektron-fonon-kopplingens (energiberoende) styrka i supraledare. BCS-teorin har utvecklats så in i detalj att tunnelstrukturer kan beräknas med en noggrannhet av ca 1% - en remarkabel framgång. För en supraledare med stark koppling måste man ta hänsyn till att växelverkan och energigapet är komplexa, energiberoende storheter. Självenergin, och livstiden hos

excitationen påverkas då potentialens retarderade natur beaktas.

Tunnelexperimenten mäter tillståndstätheten för excitationerna,

$$N_s(E) = N(0)\ \mathrm{Re}\ \{\ |E|/(E^2-\Delta^2(E))^{\frac{1}{2}}\ \}$$

Genom $\Delta(E)$ får man information om de faktorer som orsakar gapparameterns energiberoende. Exempel på resultat ges i C-L-artikeln. En bättre och mer detaljerad beskrivning av teorin bakom effekterna ges i Schrieffers artikel. Han, Scalapino och Wilkins, utförde de första kvantitativa jämförelserna teori/experiment. McMillan utvecklade teorin och tillsammans med Rowell förfinade han analysen av tunnelexperimenten. För en sammanfattning se McMillan och Rowells kapital i Parks bok "Superconductivity".

VIII.9. Tunnelspektroskopi. Föroreningar i barriären.

Elektroner kan spridas i barriären under tunnelprocesser. Inelastiska spridningar exciterar t ex vibrationer och rotationer hos molekyler, som ligger i barriärskiktet. Effekten har gett upphov till ett fält under utveckling - inelastisk tunnelspektroskopi. Genom att mäta energiförlusterna associerade med tunnelstrukturerna, vilka motsvarar spänningen minus gapspänningen, kan absorberade molekylers nivåer bestämmas. För närmare detaljer hänvisas bl a till "Tunneling Spectroscopy" (P.K. Hansma, ed. Plenum, 1982). Ett exempel på inelastisk tunneling ges i figur VIII.1, där det också ges en jämförelse med andra typer av spektroskopier.

VIII.10. Punktkontakt. Vakuumtunnling.

Punktkontakter, fins vässade spetsar drivna i en supraledare (ev med oxid på ytan), har använts som Josephsonövergångar - i ett litet område övrskrids kritiska strömmen. Även för en-elektron tunnling har punktkontakter använts, t ex för fononstudier och vid inelastisk tunnelspektroskopi.

I början av 80-talet har det utvecklats en metod, som bygger på tunnling i vakuum av elektroner från en fin spets till en metallyta. Spetsens läge (x-,y- och z-led) styrs av piezoelektriska kristaller. Tunnelströmmen är exponentiellt beroende av avståndet mellan spets och platta. Små förändringar i detta avstånd, t ex vid atomära steg i underlaget, ger en märkbar ändring i tunnelströmmen. Ändringen kopplas tillbaka och styr spetsens höjd över plattan så att man får en konstant ström. Om ytan innehåller områden med olika utträdesarbeten så fås också en ändring av tunnelströmmen. Absorberade atomer och molekyler på ytan ger också utslag. Metoden väntas få stor betydelse för mikroskopiska ytstudier. Det skall bli spännande att se vad som kommer ut de närmaste åren.

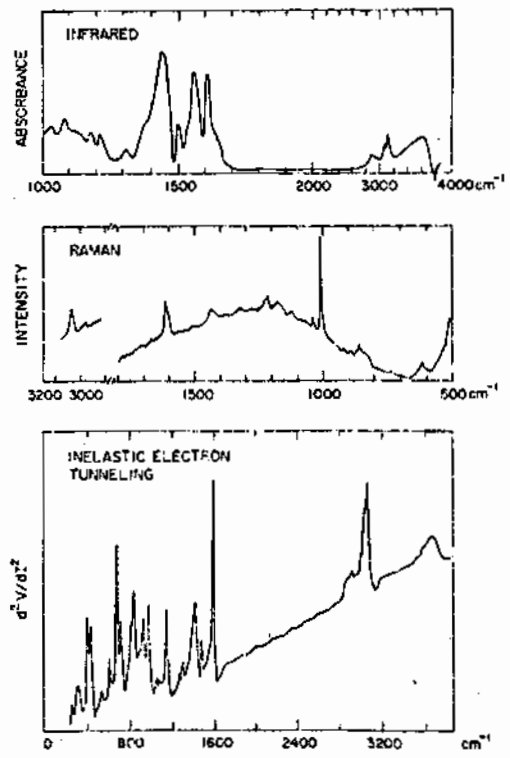

Fig. VIII.1 *Jämförelse mellan IR-, Raman- och inelastisk tunnelspektroskopi. Samma system, benzaldehyd på aluminiumoxid har studerats.*

III. DENSITY OF STATES BY TUNNELING MEASUREMENTS

The most powerful experimental method for studying the density of states in a superconductor is probably the electron tunneling technique discovered by Giaever (*48*). By this technique the tunneling current between two metals separated by a very thin insulator is measured as a function of the applied voltage, and from this the density of states as a function of energy is rather easily deduced. The simplicity of the method and the wealth of information it yields have led to many tunneling measurements, whose results constitute perhaps the most detailed comparison of the BCS theory with experiment. To allow the discussion of tunneling measurements, the semiphenomenological theory of tunneling will be briefly summarized. The purpose here is to use the summary of the theory as a means of coherently presenting results which are useful for comparison with experiments. The microscopic theory of tunneling and many specialized topics in tunneling theory are discussed at length in other chapters. The development follows Giaever and Megerle (*49*) and Shapiro et al. (*50*); and the form and presentation rely heavily on the excellent review article of Douglass and Falicov (*51*), who present other more detailed results.

A. Theory of Tunneling

The semiphenomenological theory of tunneling introduced by Giaever and Megerle (*49*) is essentially a one-dimensional model which assumes that the quasi-particles can be treated as independent Fermi–Dirac particles occupying a given state of energy ϵ with a probability $f = [1 + \exp(\beta\epsilon)]^{-1}$. The tunneling

current from metal 1 to metal 2 is assumed to be proportional to the density of occupied states at a given energy in metal 1 and to the density of unoccupied states in metal 2, at the same energy. This current is also assumed to be proportional to the probability for a given quasi-particle of this energy to tunnel through the barrier. When integrated over all energies this gives

$$i_{12} = (2\pi/\hbar)\int_{-\infty}^{\infty} |M|^2 \rho_1 f_1 \rho_2 (1 - f_2)\, d\epsilon$$

where M is the matrix element between states of equal energy in the two metals. By subtracting a similar expression for the current from metal 2 to metal 1, we obtain for the net current

$$I = A\int_{-\infty}^{\infty} |M|^2 \rho_1 \rho_2 (f_1 - f_2)\, d\epsilon \tag{10}$$

Such an analysis of electron tunneling originated with Sommerfeld and Bethe (*52*) and has been applied to many problems: a presentation and extension of their work was given by Holm (*53*). More recently Esaki (*54*) has used it successfully to describe tunneling currents in degenerate semiconductor junctions.

To adapt the analysis to tunneling with superconductors the following assumptions were made:

1. The density of states in a normal metal is a constant, $\rho_n = N(0)$.
2. The density of states in a superconductor ρ_s at $T = 0°K$ is given by the BCS relation:

$$\rho_s = \begin{cases} N(0)\dfrac{|\epsilon|}{\sqrt{\epsilon^2 - \Delta^2}} & |\epsilon| \geq \Delta \\ 0 & |\epsilon| < \Delta \end{cases} \tag{11}$$

3. The matrix element M is independent of energy in the region of interest and is independent of whether the metals are superconducting or not.
4. The difference between the Fermi energies of the two metals equals the difference in electrical potential, V.

Measuring the energy in electron volts from the Fermi energy of metal 1 the tunneling current becomes

$$I = A\int_{-\infty}^{\infty} \rho_1(\epsilon)\, \rho_2(\epsilon + V)[f(\epsilon) - f(\epsilon + V)]\, d\epsilon \tag{12}$$

where $A = (2\pi e/\hbar)|M|^2$. When both metals are normal, Eq. (12) reduces to

$$I_{nn} = AN_1(0)\, N_2(0)\int_{-\infty}^{\infty} [f(\epsilon) - f(\epsilon + V)]\, d\epsilon$$

At low temperatures and voltages ($1 \ll \beta E_F$, $V \ll E_F$) the integral is easily

evaluated and gives

$$I_{sn} = C_n V \tag{13}$$

where the constant, $C_n = AN_1(0)N_2(0)$, is the conductance for normal–normal tunneling. The linearity of this relation for Al–Al_2O_3–metal tunnel junctions was demonstrated by Fisher and Giaever (*55*) to hold for voltages up to about one-tenth of the oxide barrier height and covers the voltage range of present interest.

1. Superconductor–Normal Metal Tunneling

When metal 1 is superconducting and metal 2 is normal, Eq. (12) gives

$$I_{sn} = C_n \int_{-\infty}^{\infty} \rho_s [f(\epsilon) - f(\epsilon + V)]\, d\epsilon \tag{14}$$

If we differentiate this expression with respect to the applied voltage, we obtain

$$\frac{dI_{sn}}{dV} = C_n \int_{-\infty}^{\infty} \rho_s(\epsilon) \left(\frac{\beta \exp[\beta(\epsilon + V)]}{\{1 + \exp[\beta(\epsilon + V)]\}^2} \right) d\epsilon \tag{15a}$$

The second factor in this integral is a bell-shaped function which is symmetrical about its maximum, which is located at $\epsilon = -V$. The magnitude of this maximum is proportional to $1/T$ and at $T = 0$ the function degenerates into a delta function and

$$\left(\frac{dI_{sn}}{dV} \right)_{T=0} = C_n \rho_s \tag{15b}$$

This general result is independent of the density of states function ρ_s. For the BCS model at $T = 0$, Eq. (11) leads to

$$\left(\frac{dI_{sn}}{dV} \right)_{T=0} = \begin{cases} C_n \dfrac{|V|}{\sqrt{V^2 - \Delta^2}} & |V| \geq \Delta \\ 0 & |V| \leq \Delta \end{cases} \tag{15c}$$

If Δ is independent of energy these last equations can be integrated to give

$$I_{sn} = \begin{cases} C_n \sqrt{V^2 - \Delta^2} & V \geq \Delta \\ 0 & V \leq \Delta \end{cases} \tag{16}$$

Qualitatively this result can be understood from the density of states diagram of Fig. 4a and the resulting tunneling characteristic of Fig. 4b. At $T = 0$ there evidently can be no current from the superconductor until the applied voltage depresses the effective Fermi energy of the normal metal by an amount which is equal to Δ. At that time current should start to flow and at higher voltages the current should asymptotically approach the straight line of normal–normal

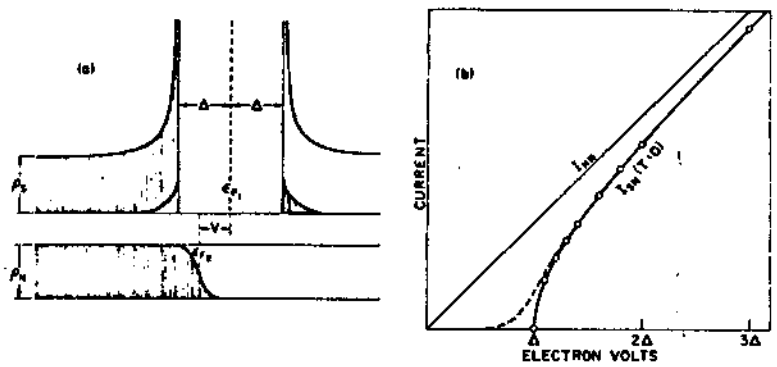

Fig. 4. (a) Schematic representation of the density of states in a superconductor–oxide–normal metal tunnel junction at a finite temperature. (b) Current as a function of voltage for such a junction at $T = 0$, $T/T_c \approx 0.2T_c$, and $T > T_c$.

tunneling. At a finite temperature well below T_c the exponential tail of the Fermi distribution always gives a finite conduction, but there remains a sudden rise for $V \approx \Delta$ as shown in Fig. 4b for $T/T_c = 0.2$.

When $T \neq 0$ the BCS conductance from Eq. (15) is

$$\frac{dI_{sn}}{dV} = C_n \left(\int_{\Delta}^{\infty} \frac{|\epsilon|}{\sqrt{\epsilon^2 + \Delta^2}} \frac{\beta \exp[\beta(\epsilon + V)]}{\{1 + \exp[\beta(\epsilon + V)]\}^2} d\epsilon + \int_{-\infty}^{-\Delta} \frac{|\epsilon|}{\sqrt{\epsilon^2 + \Delta^2}} \frac{\beta \exp[\beta(\epsilon + V)]}{\{1 + \exp[\beta(\epsilon + V)]\}^2} d\epsilon \right) \tag{17}$$

This expression for the BCS conductance has been computed numerically by Bermon (*56*) for a large range of parameters $\beta\Delta$ and βV.

The expression for the current I_{sn} in Eq. (14) has been shown by Giaever and Megerle (*49*) to be given by a series which converges rapidly for $|V| < \Delta$:

$$I_{sn} = 2C_n \Delta \sum_{m=1}^{\infty} (-1)^{m+1} K_1(m\beta\Delta) \sinh(m\beta V) \tag{18a}$$

where K_1 is the modified Bessel function of the second kind. In the low-voltage limit Eq. (18a) becomes

$$\lim_{V \to 0} I_{sn} = 2C_n \Delta \sum_{m=1}^{\infty} (-1)^{m+1} m\beta V K_1(m\beta\Delta) \tag{18b}$$

which in the low-temperature limit leads to

$$\lim_{\substack{V \to 0 \\ T \to 0}} \frac{I_{sn}}{I_{nn}} = (2\pi\beta\Delta)^{1/2} \exp(-\beta\Delta) \tag{18c}$$

2. Superconductor–Superconductor Tunneling

For this case, Eqs. (11) and (12) lead to the following expression for the tunneling current:

$$I_{ss} = C_n \int_{-\infty}^{\infty} \frac{|\epsilon|}{\sqrt{\epsilon^2 - \Delta_1^2}} \frac{|\epsilon + V|}{\sqrt{(\epsilon + V)^2 - \Delta_2^2}} [f(\epsilon) - f(\epsilon + V)]\, d\epsilon \qquad (19)$$

This result was first given by Nicol et al. (*57*), who numerically calculated sample current–voltage curves and showed that at approximately $V = \pm|\Delta_2 - \Delta_1|$ there is a logarithmic singularity in the current of magnitude:

$$I_{ss} \sim \ln|V - (\Delta_2 - \Delta_1)|$$

and at $V = \Delta_1 + \Delta_2$ there is a finite discontinuity even at $T \neq 0$,

$$\Delta I_{ss} = \frac{\pi C_n \sqrt{\Delta_1 \Delta_2}}{4} \frac{\sinh[\beta(\Delta_1 + \Delta_2)/2]}{\cosh(\beta\Delta_1/2)\cosh(\beta\Delta_2/2)} \qquad (20a)$$

These features are shown in Fig. 5b and may be understood qualitatively from considering the density of states diagram of Fig. 5a and how the product of occupied and available states of the same energy changes as the voltage is changed. At $T = 0$ Eq. (19) reduces to

$$I_{ss} = C_n \int_{-V+\Delta_2}^{-\Delta_1} \frac{|\epsilon|}{\sqrt{\epsilon^2 - \Delta_1^2}} \frac{|\epsilon + V|}{\sqrt{(\epsilon + V)^2 - \Delta_2^2}}\, d\epsilon \qquad (21)$$

Equation (21) can be integrated and expressed in terms of complete elliptic

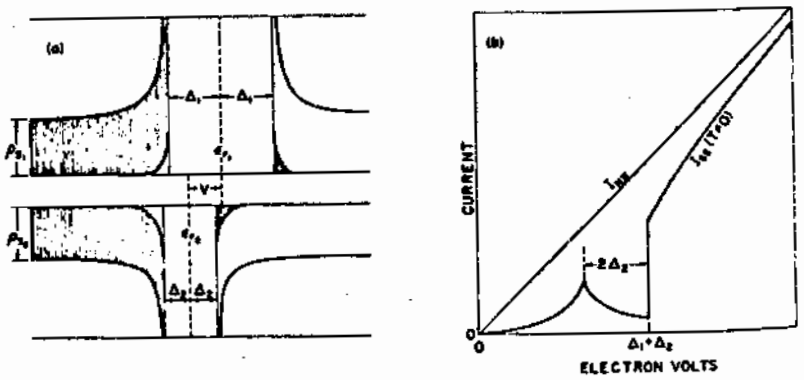

Fig. 5. (a) Schematic representation of the density of states in a superconductor–oxide–superconductor–tunnel junction at a finite temperature. (b) Current–voltage characteristic calculated from the BCS theory.

integrals (*51*). The discontinuity in the current at $V = \pm(\Delta_1 + \Delta_2)$ is at $T = 0$,

$$\Delta I = (\pi/2)\, C_n \sqrt{\Delta_1 \Delta_2} \qquad (20b)$$

When $\Delta_1 = \Delta_2 = \Delta$ and $V < 2\Delta$, Taylor et al. (*58*) have computed I_{ss} numerically and have shown that a negative resistance region ($dV/dI < 0$) should appear at $T < 0.3\Delta/k$. When $T \ll \Delta/k$ and $V < 2\Delta$, the current is well approximated by

$$I_{ss} = 2C_n \exp(-\beta\Delta)\sqrt{2\Delta/(V + 2\Delta)}(V + \Delta)\sinh(\beta V/2)\, K_0(\beta V/2) \qquad (22)$$

For $T = 0$ the discontinuity at $V = 2\Delta$ is

$$\Delta I = \pi C_n \Delta/2 \qquad (20c)$$

3. Microscopic Justification of the Semiphenomenological Theory

The semiphenomenological theory as outlined above was criticized for its rather sweeping and apparently unjustified assumptions. However, from the detailed fit that Giaever and Megerle obtained with the experimental data, it appeared that for some reason these assumptions must be justified. It is therefore satisfying that the microscopic theory of tunneling, which was developed by Bardeen (*59*), Harrison (*60*), Cohen et al. (*61*), and Prange (*62*), vindicated the original assumptions. Thus, when we compare experimental results to the semiphenomenological theory, we are also comparing them to the microscopic theory. It is appropriate to mention that the careful study of the microscopic theory did bring to light the very interesting effect of Josephson tunneling; this tunneling by superconducting pairs is found between superconductors separated by a very thin tunnel barrier. Since this effect is being treated fully in Chapter 9, the experiments discussed in this chapter will be concerned almost entirely with quasi-particle tunneling, with only brief mention of pair tunneling.

B. Basic Tunneling Experiments

One of the most attractive features of Giaever's tunneling experiments is the simplicity of the experimental method. In the original experiments a thin strip of an aluminum film was evaporated on a glass substrate. The resulting film was then oxidized for a few minutes in the laboratory atmosphere and a cross strip of some other metal such as lead was then evaporated. This technique resulted in crossed thin films of aluminum and the other metal separated by a layer of aluminum oxide about 30 Å thick. Other metals which oxidize rapidly, such as magnesium, could be substituted for the aluminum; in addition lead, tin, niobium, or tantalum could be oxidized in an atmosphere of oxygen at 50–100°C for a few minutes before the second strip was evaporated. The second metal could be anything which evaporates in vacuum, and the result was a

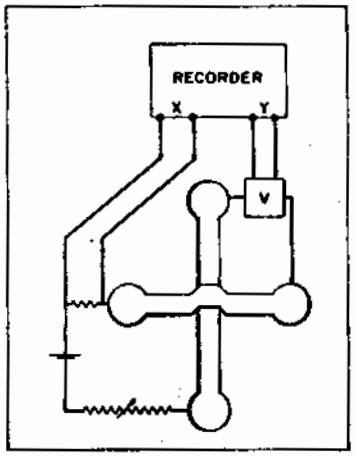

Fig. 6. Schematic diagram of a tunnel junction and the circuit used to measure current and voltage.

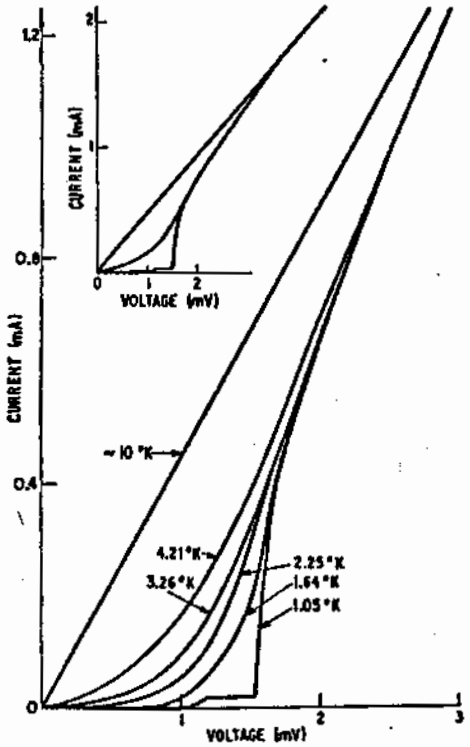

Fig. 7. Current–voltage characteristic of an Al–Al_2O_3–Sn junction at various temperatures (*49*).

four-terminal tunnel junction whose current–voltage characteristic was measured in the simple circuit shown schematically in Fig. 6.

This technique has been improved and extended in a number of ways. The oxidation can be accomplished in a more controlled way in an oxygen glow discharge. The oxide layer can also be formed by the evaporation of an insulator or the evaporation of a metal such as aluminum which can subsequently be oxidized to form the insulating layer. In addition to tunneling between thin films, it has proved possible to obtain tunneling results between bulk crystals and thin films. Levinstein and Kunzler (*63*) have developed a technique whereby a needle-like probe of niobium, tantalum, or aluminum is oxidized and used as a small area probe to obtain tunneling characteristics on a bulk sample of unoxidized metal. In the measurement of tunneling characteristics circuits have been developed to measure and plot the first and second derivatives of the current–voltage curves. These derivative plots are very useful in comparing the results with theory and have yielded a tremendous amount of detailed information. The techniques of sample preparation and circuitry have been greatly

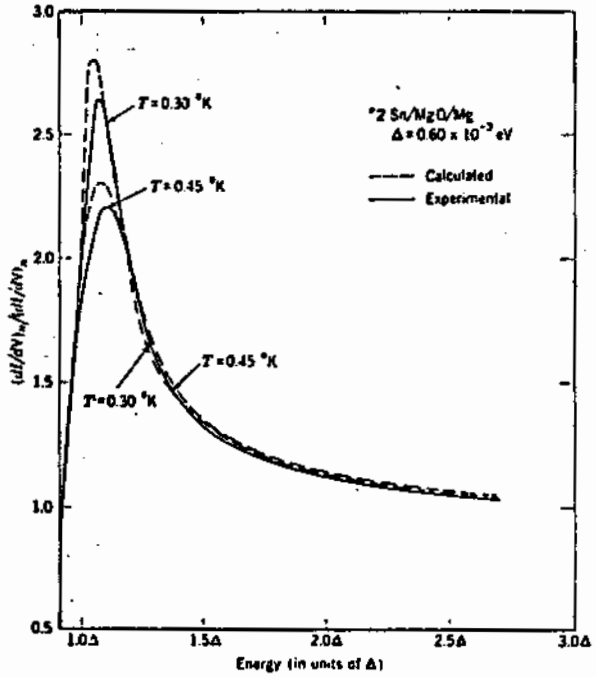

Fig. 8. Experimental and calculated relative conductance curves plotted vs. the normalized energy for two different temperatures. The BCS density of states was used in the calculation (*64*).

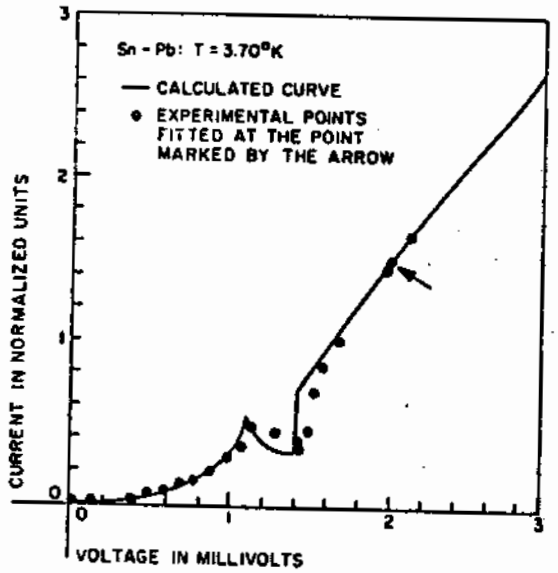

Fig. 9. Measured values of the current and voltage of a Sn–Pb tunnel junction as compared with the curve calculated from the BCS theory (*50*).

developed and are treated in detail in Chapter 11, but in spite of this development in the sophistication and power of tunneling measurements, the basic simplicity of the method remains.

Figure 7 shows one of the original tunneling curves obtained by Giaever and Megerle (*49*). The striking thing about these curves is their resemblance to what we expect from the semiphenomenological theory. At temperatures well below the transition temperature of lead but above that of aluminum the tunnel current remains low until $eV \approx \Delta_{Pb}$; here the current rises rapidly and then approaches the normal state asymptotically at higher voltages. Below the aluminum transition temperature, the curves are readily understood on the basis of the diagram of Fig. 4a, which implies: the initial rapid rise in current, the negative resistance region about equal to the gap width in aluminum, $2\Delta_{Al}$, and subsequent very rapid rise near $\Delta_{Pb} + \Delta_{Al}$. Figure 8 shows the relative conductance of a Mg–MgO –Sn junction measured by Giaever et al. (*64*) compared with the BCS theory; the agreement is excellent provided we use the measured energy gap in place of $3.53kT_c$. For superconductor–superconductor tunneling Shapiro et al., (*50*) show in Fig. 9 their measured curves for lead–tin junctions as compared with numerical calculation based on the BCS theory [Eq. (19)]. The curves are normalized at the point indicated and except for a blurring of the predicted features the general character of the curves, including the negative resistance

TABLE III

Measured Values of $2\Delta(0)/kT_c$
(BCS) theoretical value = 3.53)

Superconductor	Tunneling measurements	Ref.	Thermodynamic measurements[a]
Al	4.2 ±0.6	(*49*)	3.53
	2.5 ±0.3	(*50*)	
	2.8 – 3.6	(*68*)	
	3.37 ± 0.1	(*65*)	
Cd	3.2 ±0.1	(*65a*)	3.44
Ga			3.52, 3.50, 3.48
Hg(α)	4.6 ±0.1	(*84*)	3.95
In	3.63 ± 0.1	(*49*)	3.65
	3.45 ± 0.07	(*65*)	
	3.61	(*94*)	
La	1.65 – 3.0 (fcc)[b]	(*100*)	3.72 (fcc) (*d*-hep)
	3.2	(*100*)	
Nb	3.84 ± 0.06	(*85*)	3.65
	3.6	(*95*)	
	3.6	(*96*)	
Pb[c]	4.29 ± 0.04	(*69*)	3.95
	4.38 ± 0.01[d]	(*74*)	
Sn	3.46 ± 0.1	(*49*)	3.61, 3.57
	3.10 ± 0.05	(*50*)	
	3.51 ± 0.18	(*85*)	
	2.8 – 4.06	(*65*)	
	3.1 – 4.3	(*87*)	
Ta	3.60 ± 0.1	(*85*)	3.63
	3.5	(*95*)	
	3.65 ± 0.1	(*97*)	
Tl	3.57 ± 0.05	(*98*)	3.63
	3.9	(*94*)	
V	3.4	(*95*)	3.50
Zn	3.2 ±0.1	(*99*)	3.44

[a] The values given here were calculated from values of $\gamma T_c^2/V_M H_c^2$ (0) assuming the equation $[2\pi V_M H_c^2(0)/3\gamma T_c^2]^{1/2} = 2\Delta(0)/kT_c$.

[b] The measured tunneling results of Edelstein and Toxen (*100*) in La are very low and widely scattered and perhaps reflect the great structure sensitivity of La. Hauser's (*100a*) later measurements are higher and less scattered.

[c] Other older measurements are collected in (*51*).

[d] T_c assumed to be 7.193 °K.

region, was so similar to the predictions as to leave little doubt that the basic description of the phenomenon was correct.

Although the qualitative agreement between the BCS theory and early tunneling experiments was spectacular, the quantitative agreement was not so satisfactory. The BCS theory predicts [Eq. (3)] that in the weak-coupling limit all superconductors should have the same value for the normalized energy gap at $T=0$: $2\Delta(0)/kT_c = 3.53$. Table III lists the measured values and shows that, although there is rough agreement with theory, the deviations for some elements is large. In addition, it was found that the disagreement between theory and experiment was not to be found solely in the absolute value of the gap. In an effort to improve the agreement between the measured and calculated tunneling curves, Giaever et al. (*64*) attempted to fit their data on tin with a BCS density of states which had been averaged over a small fixed energy interval. With this empirical broadening width the calculated curves fitted the data very well, but not perfectly, even though the energy gap and the broadening width were both used as adjustable parameters. Zavaritskii (*65*), to avoid thermal broadening, measured the conductance of Pb, Sn, In, and Al at temperatures down to 0.1°K and so essentially reached the region where Eq. (16) should apply. However, the finite slope of the current discontinuity remained, and with it some ambiguity about the exact size of the energy gap. In the low-temperature limit near zero voltage Eq. (18c) predicts an exponential temperature dependence of the energy gap; Fig. 10 shows that the normalized experimental results have this temperature dependence and give an independent way of obtaining the energy gap. In the case of superconductor–superconductor tunneling the results of Shapiro agree fairly well with the discontinuity predicted by Eq. (20a) although the finite slope does not allow an exact comparison. However, even a casual inspection of the experimental curves shows that the theoretical cusp-like logarithmic singularity of Eq. (19) is not to be found on the experimental curves. In the case of identical superconductors the results of Gasparovic et al. (*66*) on a lead–lead junction are shown in Fig. 11 and compared with values numerically calculated from the BCS theory using a value of $2\Delta(T)$ adjusted to fit the experimental curve at the point shown in the figure. Again, except for the region near the gap edge, the agreement is excellent.

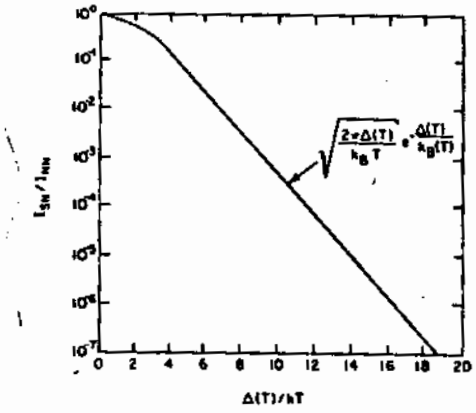

Fig. 10. Plot of the ratio I_{sn}/I_{nn} as a function of $\Delta(T)/kT$. The exponential behavior is apparent at the lower temperatures (*51*).

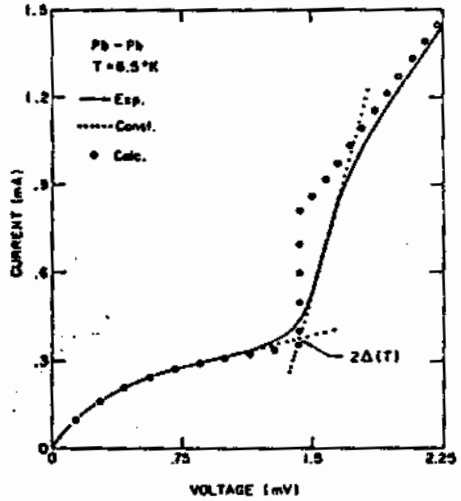

Fig. 11. Current–voltage characteristic of a lead–lead junction compared with values calculated from the strong-coupling theory for lead. Dashed lines show construction used to determine the energy gap (*66*).

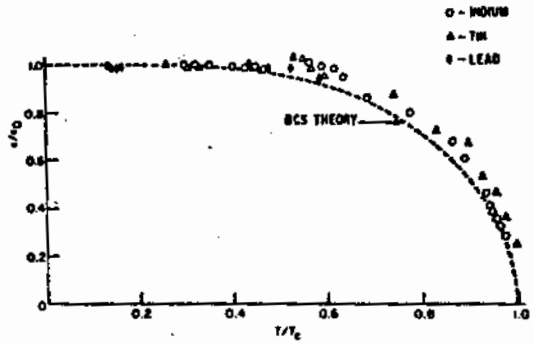

Fig. 12. Normalized measured energy gap of Pb, Sn, and In vs. temperature as compared with the BCS theory (*49*).

Figure 12 shows measurements of the temperature dependence of the energy gap in thin films of lead, tin, and indium obtained by Giaever and Megerle (*49*). Although the scatter of the measurements is large, there is good general agreement with the BCS theoretical values as calculated by Mühlschlegel (*67*) for the weak-coupling limit. Figure 13 shows later measurements of Douglass and Meservey (*68*) on aluminum thin films. Although the structure and thickness of the films were evidently important in determining the absolute value of the gap, the temperature dependence agreed with BCS up to a reduced temperature

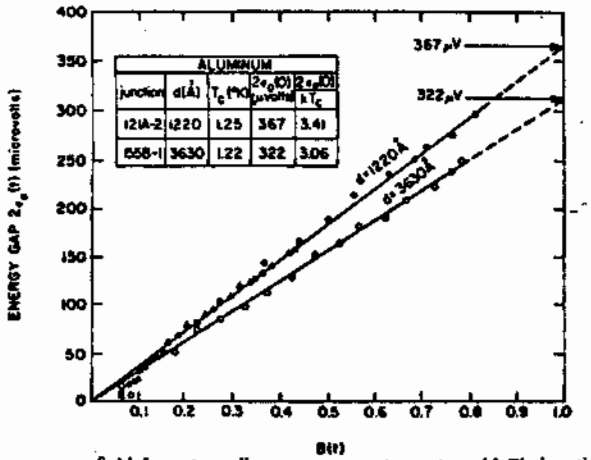

Fig. 13. Energy gap of Al from tunneling measurements on two Al–Pb junctions vs. the theoretical BCS function (*68*).

$T/T_c = 0.993$; the deviation near T_c is probably not significant because of the increasing ambiguity in obtaining the gap from experimental data as T_c is approached.

It is to be noted that quantitative agreement was found only when the results were normalized in some way. The absolute value of the energy gap deviates from the BCS model prediction of $3.53kT_c$ by as much as 30% in the case of mercury. There was even considerable scatter in the values obtained for the same metal from different thin-film samples; in the case of tin films Zavaritskii (*65*) found values of $2\Delta(0)/kT_c$ ranging from 2.8 to 4.06. In some instances the discrepancy in the energy gap between different samples has been shown to be associated with anisotropy, a subject that will be discussed in more detail in Section III.E. It should be pointed out that most of the results in Table III were obtained from thin-film samples whose properties may depend on strains caused by the substrate, on gaseous impurities, and on surface effects. Although these thin-film results are not equivalent to measurements on single crystals, the larger

disagreements in Table III with the simple BCS model cannot be attributed primarily to thin-film effects.

The smearing of the predicted singularities and discontinuities is disappointing in itself; in addition, it makes the determination of the energy gap somewhat ambiguous. For large energy gaps at low reduced temperature this broadening introduces an error of perhaps only 2%. On the other hand, near the transition temperature or the critical field the value of the energy gap as judged from the tunneling characteristics becomes very uncertain. For these cases an understanding of the broadening mechanisms is essential before a precise comparison with theory is possible.

C. Effect of the Discrete Phonon Spectrum

More startling than these broadening effects was the observation by Giaever et al. (*64*) that the relative conductance curve for lead (Fig. 14) exhibits qualitative features which were not predicted by the simple BCS model. This figure

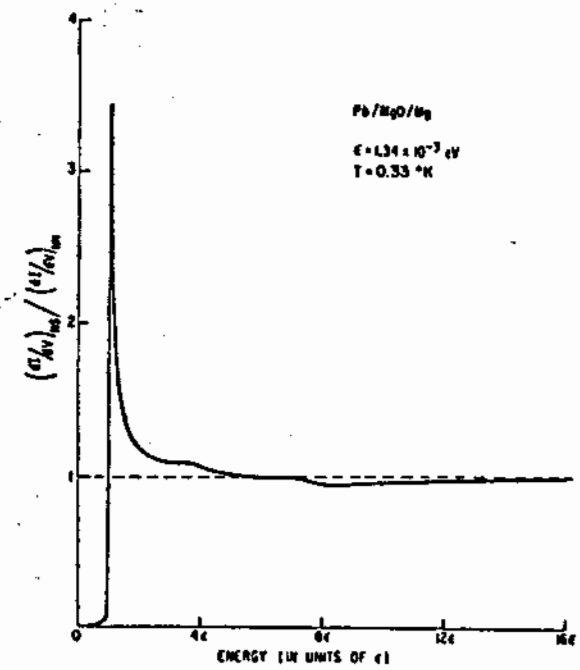

Fig. 14. Differential conductance of a Pb–Mg junction vs. voltage, showing the superconducting density of states of Pb (*64*).

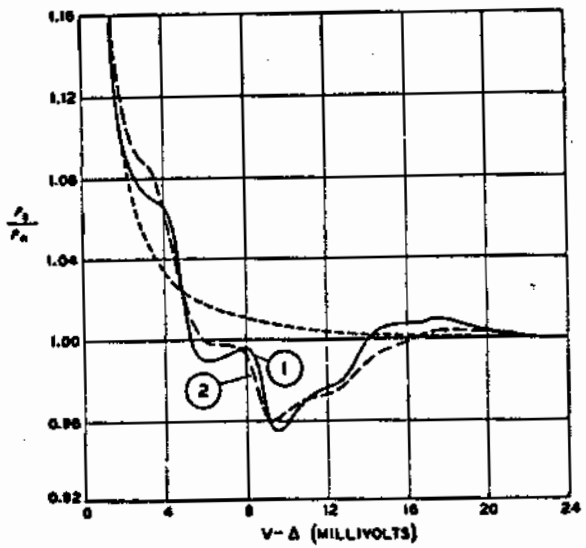

Fig. 15. Comparison of (1) the density of states vs. energy as calculated by Schrieffer et al. (solid line); (2) the measured tunneling characteristic (long-dashed line); and the BCS theory (short-dashed line) (*70*).

shows additional structure in the density of states curve and shows that the conductance in the superconducting state at high energy (or voltage) is actually less than that for the normal state. It was pointed out by the above authors that the crossover point was approximately at the Debye energy.

The discovery of structure in the density of states of lead aroused much interest because the most natural explanation was that it reflected the nature of the phonon spectrum. This was particularly plausible in lead because the Debye energy was so low that lead had been expected to deviate most strongly from the BCS constant-interaction model. Rowell et al. (*69*), using a more sensitive method of measuring dI/dV, succeeded in resolving considerable detail in the relative conductance curves in a lead–aluminum tunnel junction (Fig. 15).

The effect on the density of states of a simple but realistic phonon spectrum has been calculated by Schrieffer et al. (*70*). Using the Eliashberg (*8*) treatment of a retarded interaction, these authors showed that the density of states, as measured by tunneling experiments, could be represented by the simple expression

$$\rho_s = \rho_n \operatorname{Re}\left[\frac{\epsilon}{\sqrt{\epsilon^2 - \Delta^2(\epsilon)}}\right] \tag{23}$$

which is the same as the BCS expression except that the gap function, Δ, is complex and a function of the energy. The complex energy gap indicates that

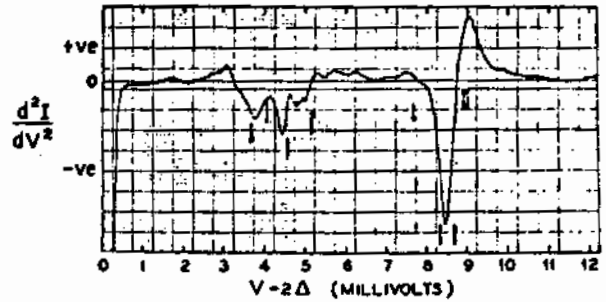

Fig. 16. (d^2I/dV^2) vs. $(V-2\Delta)$ for a Pb–Pb junction at 1.3°K. Arrows indicate the bias for Van Hove singularities expected from neutron measurements of the phonon spectrum (*74*).

in the high-energy region the damping of the quasi-particles becomes important. Using this density of states expression and a phonon spectrum consisting of two Lorentzian broadened peaks (as shown at the bottom of Fig. 15) a theoretical tunneling characteristic was calculated. The position and width of the phonon peaks were chosen to approximately fit the phonon spectrum observed in neutron scattering experiments by Brockhouse et al. (*71*), and the electron–phonon coupling constant was adjusted to give the experimental value of $\Delta(0)$. Figure 15 shows that this calculation reproduces the tunneling results not only near the phonon peaks but also at higher energies where the effect of harmonics of the phonon frequencies is observed. Discrepancies between the phonon density of states derived from neutron scattering and tunneling have been noted by Dynes et al. (*71a*) and attributed to the force constant model assumed in analyzing the tunneling data.

It was also discovered by Rowell et al. (*69*) that by observing the second derivative d^2I/dV^2 of a lead–lead junction much more structure in the effective density of states was revealed, as shown in Fig. 16. Scalapino and Anderson (*72*) attributed this structure to variations in the density of states caused by critical points (*73*) (maxima, minima, or saddle points) of the phonon spectrum, and, indeed much of the observed structure can be correlated in this way with neutron scattering measurements of the phonon spectrum. Other measurements of tin, indium, and thallium all support these general findings, although the knowledge of the phonon spectra is not complete enough to allow a complete analysis. In fact, McMillan and Rowell (*74*) have shown that this method in reverse provides a very powerful technique of determining the phonon spectrum from the observed effective density of states, and Rowell and Kopf (*75*) have applied the methods to lead, tin, indium, and thallium. The detailed correlation between the density of states and the phonon spectrum is very strong evidence that the attractive interaction between electrons is a retarded one involving phonons.

Chapter 21

Single-Particle Tunneling in Superconductors*

J. R. Schrieffer

Department of Physics
University of Pennsylvania
Philadelphia, Pennsylvania

INTRODUCTION

Tunneling experiments reveal a good deal about the nature of the superconducting state. Here we consider only single-particle tunneling. In this case one can summarize the results in terms of an effective tunneling density of states $N_T(E)$ which is analogous to the conventional density of states is normal metals and which can be compared rather directly with experiment. In the case of multiparticle tunneling, more complicated effects occur (e.g., the Josephson effect) which are treated elsewhere in this volume.

To treat single-particle tunneling we consider the idealized tunneling experiment shown in Fig. 1. Here metals A and/or B may be in the normal or superconducting state, depending on the temperature, applied magnetic field, etc. Ideally, one would like to predict the current I flowing through the junction as a function of the DC applied bias V. For convenience we

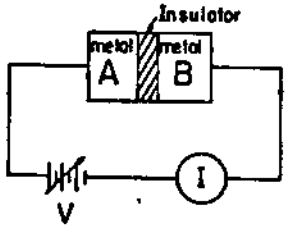

Fig. 1. The tunneling experiment.

* This work was supported in part by the Advanced Research Projects Agency.

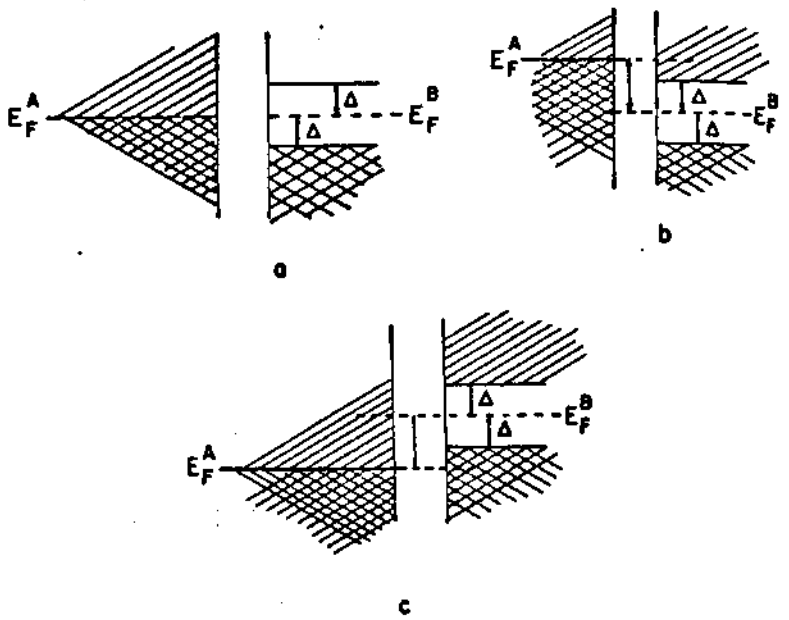

Fig. 2. (*a*) A normal metal-superconductor tunnel junction at zero bias described by the semiconductor model of the excitation spectrum of the superconductor. A normal-super junction with a bias V applied, leading to electron flow from A to B in (*b*) and electron flow from B to A (hole flow from A to B) in (*c*).

define V to be the electron charge $(-e)$ times the actual applied voltage. We first consider the case in which metal A is normal and metal B is superconducting. The semiconductor-type energy level diagram can be used to describe this case if one is careful to use the diagram correctly. For $V = 0$ the Fermi levels $E_F^{(A)}$ and $E_F^{(B)}$ are equal, as shown in Fig. 2(*a*). Considering for the moment the temperature $T = 0$, quasiparticles can flow between A and B only if V is greater than Δ [Fig. 2(*b*)] or less than $-\Delta$ [Fig. 2(*c*)], corresponding to quasielectron and quasihole flow into the superconductor, respectively.

An alternate way of discussing tunneling is in terms of the energy-momentum diagrams, shown in Fig. 3 for $T = 0$. In the normal metal one can speak in terms of the Landau theory of a Fermi liquid, in which the states of the Fermi liquid are in one-to-one correspondence with the states of the Fermi gas. At $T = 0$ all states with $|p| > p_F$ are occupied and those with $|p| < p_F$ are empty. In the normal phase an excited state can be

described in terms of electrons in states with $|p| > p_F$ having positive excitation energies $\varepsilon_p^{(A)} \equiv E_p^{(A)} - E_F^{(A)} > 0$ and holes in states $|p| < p_F$ also having *positive* excitation energies, $-\varepsilon_p^{(A)} \equiv -(E_p^{(A)} - E_F^{(A)}) > 0$. Clearly, the total excitation energy is correctly given by the sum of these positive "elementary" excitation energies. This situation is illustrated in Fig. 3(*a*). Due to the sharpness of the Fermi surface at $T = 0$, as illustrated by the dotted curve of Fig. 3(*b*), one can only add electrons above the Fermi surface ($|p| > p_F$) and add holes below ($|p| < p_F$).

The situation is somewhat more complicated in a superconductor. As a consequence of the pairing interaction, the mean occupation numbers $\langle n_k \rangle$ of the Landau theory do not change abruptly near the Fermi surface even at $T = 0$, in contrast to a normal metal [see Fig. 3(*b*)]. As a result of the smearing of the Fermi surface in the superconducting phase, one cannot, as in the normal phase, think of a single-particle energy versus momentum curve in which all states below a Fermi surface in k space are occupied at $T = 0$ and all above it are empty. Instead, one should think of the excitation energy curves directly, i.e., the energy required to add an electron to the system (or remove an electron from the system) such that the total momentum of the system is increased (or decreased) by k. These curves (addition of a quasielectron or a quasihole) are shown in Fig. 3(*c*). Again the excitation energies are *positive* for both types of excitations, although we plot the quasielectron energy $E_k^{(e)}$ positive upward and $E_k^{(h)}$ positive downward to make as close contact as possible with the conventional E–k curve for a normal metal. In a superconductor the minimum energy to insert a quasi particle is $\Delta = E_{k_F}^{(e)} = E_{k_F}^{(h)}$. Now, as Δ goes to zero, the probability that one can inject an electron into a state with $|k| < k_F$, or a hole into a state with $|k| > k_F$, tends to zero, since in this limit the smearing of the Fermi surface goes to zero. From Fig. 3(*c*), one sees that the hole curve for $|k| < k_F$ and the electron curve for $|k| > k_F$ smoothly join as $\Delta \to 0$, giving just the excitation curve, Fig. 3(*a*), of the normal metal. The electron curve for $|k| < k_F$ and the hole curve for $|k| > k_F$ in Fig. 3(*c*) are irrelevant in this limit, since the probability for injection into these states vanishes as $\Delta \to 0$.

We note that for a given electron excitation energy there is a unique p (in our one-dimensional plot) in the normal metal, while there are *two* k states in the superconductor having the *same* energy. The same situation holds for the holes. This twofold degeneracy of states in the superconductor is of great importance in determining the tunneling characteristic.

Therefore the states above the energy gap in the semiconductor description (Fig. 2) correspond to the electron excitation curve of Fig. 3(*c*), and

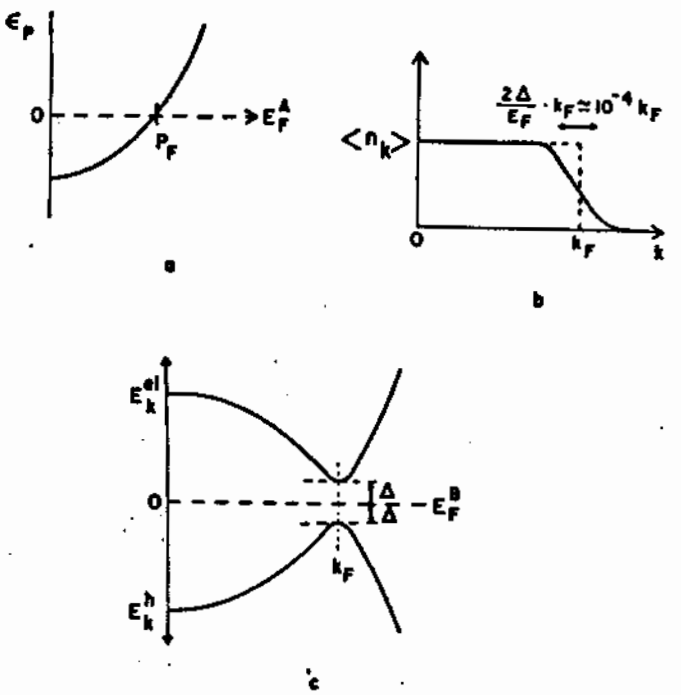

Fig. 3. (*a*) Energy versus momentum curve for electrons in a normal metal. (*b*) The average occupation numbers $\langle n_k \rangle$ at zero temperature plotted as a function of k for a normal metal (dashed) and for a superconductor (solid). The pairing interactions smear the Fermi surface of a superconductor even at $T = 0$. (*c*) The quasielectron and quasihole excitation energies plotted as functions of momentum for a superconductor. Quasihole energies are plotted positively downward. Due to the smearing of the Fermi surface, even at $T = 0$ a quasielectron or a quasihole can be added to any k state without violating the Pauli principle, as opposed to the situation in a normal metal.

one sees that *all* k states enter, both $|k| > k_F$ and $|k| < k_F$. The states below the energy gap in the semiconductor description correspond to the hole excitation curve of Fig. 3(*c*), and again *all* k states enter. This situation is in sharp distinction to real semiconductors, for which the states above and below the gap are truly of different character, arising from different single-particle energy bands. In applying the semiconductor diagrams to superconductors this feature must be kept in mind.

CALCULATION OF THE TUNNELING CURRENT

To calculate the current, we use the Hamiltonian formalism of tunneling as discussed first by Bardeen, and as formulated by Cohen, Falicov, and Phillips. The Hamiltonian has been justified to first order in the tunneling matrix element by Kadanoff using a Green's function treatment. Since we are interested only in terms of leading order in this matrix element, the Hamiltonian formalism suffices for our purposes. In this scheme one writes

$$H = H_A + H_B + H_T, \tag{1}$$

where H_A and H_B are the full many-body Hamiltonians for the isolated metals A and B and H_T represents a one-body coupling term which transfers single electrons between A and B. In terms of the creation and destruction operators for Bloch states in A (labeled ps) and in B (labeled ks) one has

$$H_\perp = \sum_{p,k,s} (T_{pk} c_{ks}^+ c_{ps} + T_{pk}^* c_{ps}^+ c_{ks}), \tag{2}$$

where T_{pk} is the tunneling matrix element, often approximated by the WKB expression. For a truly planar insulating layer the component of the momentum parallel to the surface is conserved.

The tunneling rate is given to order T^2 by the golden rule

$$w_{i\to f} = (2\pi/\hbar)\,|M_{if}|^2\,\delta(\mathscr{E}_i - \mathscr{E}_f), \tag{3}$$

where i and f label the initial and final eigenstates of the zero-order Hamiltonian $H_A + H_B$ and M_{if} is the corresponding matrix element of H_T. If $V > 0$, so that electrons flow from A to B, let the states be

$$\begin{aligned} |i\rangle &= |0\rangle_A\ |0\rangle_B, \\ |f\rangle &= |\overline{ps}\rangle_A\,|ks\rangle_B, \end{aligned} \tag{4}$$

where $|0\rangle_A$ is the ground state of A, $|\overline{ps}\rangle_A$ is the eigenstate of A with a hole in ps (holes will be represented by a bar), $|0\rangle_B$ is the ground state of B, and $|ks\rangle_B$ is the eigenstate of B with a quasielectron in ks. This process is illustrated in Fig. 4, where k can be either k_1 or k_2. Energy conservation [arising from the delta function in Eq. (3)] requires that

$$\mathscr{E}_i - \mathscr{E}_f = \epsilon_p + V - E_k = 0. \tag{5}$$

Since $\epsilon_p < 0$ and $E_k > \Delta$, we see the process takes place only if $V > \Delta$.

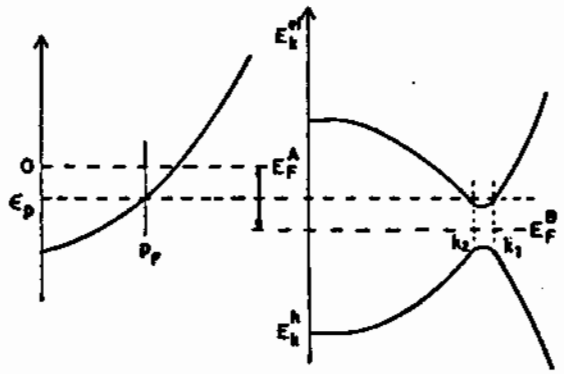

Fig. 4. A normal–super junction biased for electron flow from A to B, as described in the energy–momentum picture. Note the twofold degeneracy of the superconductor excitations. This degeneracy plays an important role in determining the shape of the tunneling characteristic.

The matrix element is

$$M_{if} = \langle f\,|\,H_T\,|\,i\rangle = T_{pk}\langle \overline{ps}\,|\,c_{ps}\,|\,0\rangle_A \langle ks\,|\,c_{ks}^+\,|\,0\rangle_B. \tag{6}$$

Now, $\langle ps\,|\,c_{ps}\,|\,0\rangle_A = 1$, since we are describing the normal metal in terms of a single-particle Bloch scheme, while the pairing theory gives

$$\langle ks\,|\,c_{ks}^+\,|\,0\rangle_B = u_k = \left[\frac{1}{2}\left(1 + \frac{\epsilon_k}{E_k}\right)\right]^{1/2}, \tag{7}$$

with ϵ_k the Bloch state energy measured with respect to $E_F^{(B)}$. Therefore the tunneling rate from i to f is

$$w_{i\to f} = (2\pi/\hbar)|\,T_{pk}\,|^2 u_k^2\,\delta(\epsilon_p + V - E_k), \tag{8}$$

while the total tunneling rate for creation of a hole in p is

$$w_p = \sum_k (2\pi/\hbar)\,|\,T_{pk}\,|^2 u_k^2\,\delta(\epsilon_p + V - E_k). \tag{9}$$

From the pairing theory we know that

$$E_k^{(e)} = E_k^{(h)} = (\epsilon_k^2 + \Delta^2)^{1/2}. \tag{10}$$

If k_1 satisfies the energy conservation condition,

$$\varepsilon_p + V = E_k, \tag{11}$$

then so does k_2, where $\varepsilon_{k_2} = -\varepsilon_{k_1}$, since from Eq. (10) $E_{k_2} = E_{k_1}$. Since $\varepsilon_{k_\perp} = 0$, we see that k_1 and k_2 are on opposite sides of the Fermi surface. Summing the contributions from these two degenerate states and assuming T_{pk} is essentially independent of k for the k's in question (this restriction is easily removed) one finds

$$\begin{aligned} w_p &= (2\pi/\hbar) \sum_k |T_{pk}|^2 u_k^2 \, \delta(\varepsilon_p + V - E_k) \\ &= (2\pi/\hbar) |T_{pk}|^2 \sum_{k\perp} \delta(\varepsilon_p + V - E_{k\perp}), \end{aligned} \tag{12}$$

where momentum conservation forces the components of p and k_1 parallel to the interface to be equal, and $k_{1\perp}$ is the component of k_1 perpendicular to the interface. In (12) the sum is over k_1 above the Fermi surface ($|k_1| > k_F$), since for each k_1 above the Fermi surface there is a term k_2 in the sum from below the Fermi surface such that $u_{k_1}^2 + u_{k_2}^2 = 1$. Thus it is the twofold degeneracy of the levels in the superconductor which leads to the of disapperrance the quasiparticle matrix element factor u_k^2 from the sum (12) if one writes the result in terms of a sum over states above the Fermi surface. It is conventional to rewrite (12) in terms of the density of tunneling states N_T by

$$\begin{aligned} \sum_{k\perp} \delta(\varepsilon_p + V - E_k) &= \int \nu(k_\perp) \, \delta(\varepsilon_p + V - E_k) \, dk_\perp \\ &= \int \nu(k_\perp) \frac{m}{k_\perp} \frac{d\varepsilon_k}{dE_k} \delta(\varepsilon_p + V - E_k) \, dE_k \\ &= \left[\nu(k_\perp) \frac{m}{k_\perp} \frac{d\varepsilon_k}{dE_k} \right]_{Ek = \varepsilon_p + V} \equiv \nu(k_\perp) \frac{m}{k_\perp} \frac{N_T(\varepsilon_p + V)}{N(0)}. \end{aligned} \tag{13}$$

Here N_T is defined in terms of the density of states at the Fermi surface in the normal metal, $N(0)$, by

$$N_T(E) = N(0) \, d\varepsilon/dE = N(0)[|E|/(E^2 - \Delta^2)^{1/2}]. \tag{14}$$

From Fig. 4 it is clear that dI/dV is proportional to the tunneling rate for electrons at the Fermi surface of A, i.e., $\varepsilon_p = 0$, so that

$$dI_{NS}/dV = \alpha N_T(V) = \alpha N(0)[|V|/(|V|^2 - \Delta^2)^{1/2}], \tag{15}$$

where α is a constant involving the average of $|T|^2$ and the $k_\perp$ factors of (13). If B is normal, Δ is zero and one has from (15)

$$dI_{NN}/dV = \alpha N(0). \tag{16}$$

Therefore one has the remarkably simple relation for the normalized conductance

$$g(V) \equiv \frac{dI_{NS}/dV}{dI_{NN}/dV} = \frac{|V|}{(V^2 - \Delta^2)^{1/2}}. \tag{17}$$

This is just the result one would derive if one naively used the semiconductor model with the conventional density of states for quasiparticles given by the pairing theory, $N(0)|E|/(E^2 - \Delta^2)^{1/2}$.

Enheartened by this simple result, one might assume that if Δ varies with k, the appropriate generalization of the expression (17) for g would be

$$g(V) = \frac{d\varepsilon}{dE}\bigg|_V = \frac{d[E^2 - \Delta^2(E)]^{1/2}}{dE}\bigg|_V = \frac{|E - \Delta(d\Delta/dE)|}{[E^2 - \Delta^2(E)]^{1/2}}\bigg|_{E=V}. \tag{18}$$

This is in fact incorrect; as we shall see below, and the correct expression is

$$g(V) = \mathrm{Re}\{|V|/[E^2 - \Delta^2(E)]^{1/2}\}, \tag{19}$$

where Δ can in general be complex.

For the reverse bias case holes flow from A to B (i.e., electrons from B to A) and the calculation proceeds just as above if one interchanges creation and destruction operators. Thus the matrix element entering from the superconductor is

$$\langle \overline{ks} | c_{ks} | 0 \rangle = v_k = \left[\frac{1}{2} \left(1 - \frac{\varepsilon_k}{E_k} \right) \right]^{1/2}. \tag{20}$$

By squaring and summing on k one again has the twofold degenerate states k_1 and k_2, such that $v_{k_1}^2 + v_{k_2}^2 = 1$ and v_k^2 drops from the tunneling expression if k is summed only above the Fermi surface, as in the $V > 0$ case. One finds that (17) holds for either sign of V.

If one carries out the analysis for $T \neq 0$, other processes can occur—for example, thermally excited electrons in A can tunnel to states in B above the gap edge even for $|V| < \Delta$. Alternatively, certain tunneling processes allowed at $T = 0$ are forbidden by the Pauli principle, since some of the final states may be already occupied by thermally excited quasiparticles. When these effects are carefully worked out all the u^2 and v^2 factors disappear and one comes back to the simple semiconductor picture

for the simple single-particle tunneling effect, as Giaever initially assumed in explaining his pioneering experimental results.

MANY-BODY FORMULATION OF TUNNELING THEORY

Early tunneling curves of Giaever and of Rowell on normal metal–superconducting lead junctions exhibited structure not accounted for by the above theory if Δ is taken to be constant. The structure occurred at voltages corresponding to the typical energies of the transverse and longitudinal phonons of lead plus Δ. Thus one had the possibility of a direct verification of the phonon mechanism of superconductivity in metals with such anomalies. To properly treat the energy dependence of Δ, one must take account of the retarded nature of the phonon interaction between electrons, since in typical metals the sound velocity is three orders of magnitude smaller than the Fermi velocity. Fortunately, the Green's function method of many-body theory handles this problem in a simple manner.

To see how this comes about, we see from the tunneling Hamiltonian and the golden rule that the exact expression for the transition rate for an electron to be withdrawn from state ps of A and inserted with total energy $E = \epsilon_p + V$ into any state of B is proportional to

$$\sum_s |T_{ps}|^2 \sum_n |\langle n | c_{ks}^\dagger | 0 \rangle_B|^2 \delta(E - \mathscr{E}_n^{(B)}), \tag{21}$$

where the $|n\rangle$ are the exact eigenstates of H_B

$$H_B |n\rangle = \mathscr{E}_n^{(B)} |n\rangle.$$

We set the initial ground-state energy of B equal to zero and measure single-particle energies in B relative to the Fermi energy. Therefore $\mathscr{E}_n^{(B)} \geq 0$. If the energy gap were perfectly sharp, one would have $\mathscr{E}_n^{(B)} > \Delta$. We suppress the index B for now.

While (21) allows one to calculate the tunnel current in principle, in practice it is impossible to determine the exact eigenstates $|n\rangle$ and the energies $\mathscr{E}_n$. Thus we desire a method to calculate the n sum in (21) directly.

Consider the *gedanken* experiment of adding an electron in Bloch state ks to B at time zero if B were initially in its ground state $|0\rangle$. Then just after the electron has been added B is in the state

$$|ks, 0\rangle = c_{ks}^\dagger |0\rangle. \tag{22}$$

Due to the many-body interactions, $|ks, 0\rangle$ is not an exact eigenstate of H. From elementary quantum mechanics one knows that after a time t has elapsed the state evolves to

$$|ks, t\rangle = e^{-iHt/\hbar} |ks, 0\rangle. \tag{23}$$

We now ask, what is the probability amplitude that the state at t is identical to that just after the particle was added? Let us call this probability amplitude

$$\begin{aligned} iG_s^>(k, t) &= \langle ks, 0 | ks, t \rangle, \qquad t > 0, \\ &= 0, \qquad\qquad\quad t < 0. \end{aligned} \tag{24}$$

Rewriting this expression, we have for $t > 0$

$$\begin{aligned} G_s^>(k, t) &= -i\langle 0 | c_{ks} e^{-iHt/\hbar} c_{ks}^\dagger | 0 \rangle \\ &= -i \sum_n \langle 0 | c_{ks} | n \rangle \langle n | c_{ks}^\dagger | 0 \rangle \exp(-i\mathscr{E}_n t/\hbar) \\ &= -i \sum_n |\langle n | c_{ks}^\dagger | 0 \rangle|^2 \exp(-i\mathscr{E}_n t/\hbar). \end{aligned} \tag{25}$$

By taking the time Fourier transform of (25) we get

$$G_s^>(k, E) = \int_{-\infty}^{\infty} G_s^>(k, t) e^{iEt/\hbar} = \sum_n \frac{|\langle n | c_{ks}^\dagger | 0 \rangle|^2}{E - \mathscr{E}_n + i\delta}, \tag{26}$$

where $\delta = 0^+$. By using the relation for a factor occurring under an integral,

$$\frac{1}{x \pm i\delta} = \frac{P}{x} \pm i\pi\delta(x), \tag{27}$$

where P signifies the principle part, one finds the desired sum

$$A_s^>(k, E) \equiv \sum_n |\langle n | c_{ks}^\dagger | 0 \rangle|^2 \delta(E - \mathscr{E}_n) = (1/\pi) |\operatorname{Im} G_s^>(k, E)|. \tag{28}$$

For hole injection (reverse-bias tunneling) one requires a slightly different sum

$$A_s^<(k, E) = \sum_n |\langle n | c_{ks} | 0 \rangle|^2 \delta(E + \mathscr{E}_n). \tag{29}$$

This quantity can be calculated from the corresponding hole probability amplitude

$$\begin{aligned} G_s^<(k,t) &\equiv 0, && t>0 \\ &\equiv i\langle 0 \mid c_{ks}^\dagger e^{iHt/\hbar} c_{ks} \mid 0\rangle \\ &\equiv i\sum_n |\langle n \mid c_{ks} \mid 0\rangle|^2 \exp(i\mathscr{E}_n t/\hbar), && t<0 \end{aligned} \tag{30}$$

by

$$A_s^<(k,E) = (1/\pi)\,|\operatorname{Im} G_s^<(k,E)|. \tag{31}$$

We note that $A^>$ and $A^<$ are nonzero only for $E>0$ and $E<0$, respectively, for our $T=0$ case. From (24) and (30) we see that $G^> + G^<$ is the conventional time-ordered Green's function

$$G_s(k,t) = -i\langle 0 \mid T\{c_{ks}(t)c_{ks}^\dagger(0)\} \mid 0\rangle, \tag{32}$$

where

$$c_{ks}(t) = e^{iHt/\hbar} c_{ks} e^{-iHt/\hbar} \tag{33}$$

and

$$\begin{aligned} T\{A(t)B(0)\} &= A(t)B(0), && t>0, \\ &= \pm B(0)A(t), && t<0, \end{aligned} \tag{34}$$

the + and − signs referring to Bose and Fermi statistics, respectively (− in our case of electrons).

Thus the tunneling density of states is given by

$$N_T(E) = \sum_k (1/\pi)\,|\operatorname{Im} G(k,E)|, \tag{35}$$

where we suppress the spin index s. We can now use standard many-body techniques for calculating $G(k,E)$.

EXAMPLES OF GREEN'S FUNCTION FORMULATION

Free Particles

For this case it is well known that $N_T(E) = N(E)$, the density of single-particle states. However, for free particles

$$G(k,E) = 1/(E - \epsilon_k + i\delta \operatorname{sgn} E), \qquad \operatorname{sgn} E = E/|E|. \tag{36}$$

Thus from (35) we find

$$\begin{aligned} N_T(E) &= \sum_k (1/\pi)\,|-\pi \operatorname{sgn} E\,\delta(E-\epsilon_k)| = \sum_k \delta(E-\epsilon_k) \\ &= \int N(\varepsilon)\,\delta(E-\varepsilon)\,d\varepsilon = N(E), \end{aligned} \tag{37}$$

as required. For $E>0$ this gives the electron injection density of states, while for $E<0$ this gives the density of states for hole injection (since all states below the Fermi level are occupied at $T=0$).

Decaying Particles

Let us make the usual Wigner–Weisskopf assumption of a single-lifetime-type decay of the initial state, i.e.,

$$\begin{aligned} iG^>(k,t) = \langle k,0 \mid k,t\rangle &\sim \exp(-\Gamma t/\hbar)\exp(-i\epsilon_k t/\hbar), && t>0 \\ &= 0, && t<0. \end{aligned} \tag{38}$$

Then

$$G^>(k,E) = 1/(E - \epsilon_k + i\Gamma) \tag{39}$$

and the electron tunneling density of states is

$$N_T(E) = \sum_k \frac{1}{\pi}\frac{\Gamma}{(E-\epsilon_k)^2+\Gamma^2} = \int N(\varepsilon_k)\frac{\Gamma/\pi}{(E-\epsilon_k)^2+\Gamma^2}\,d\varepsilon_k \approx N(E), \tag{40}$$

where we have assumed that $N(\varepsilon_k)$ varies slowly with ε_k on the scale of the level width Γ. This shows that a finite lifetime of the final state is not expected to appreciably affect the tunneling rate. The same result holds for decaying holes.

Complex Decay Curve

For the more complicated situation in which the initial state decays through many different channels one expects many different lifetimes to enter the problem. These are included by defining the self-energy $\Sigma(k,E)$ by

$$G(k,E) = 1/[E - \epsilon_k - \Sigma(k,E)]. \tag{41}$$

In simple cases the real part Σ_1 gives the level shift and the imaginary part Σ_2 gives the decay rate associated with the interactions. In normal metals the strong electron–phonon interaction leads to large real and imaginary parts of $\Sigma(k,E)$, but Σ is slowly varying with k (i.e., $\partial\Sigma/\partial\epsilon_k \sim \Sigma/E_F$), while Σ is rapidly varying with E (i.e., $\partial\Sigma/\partial E \sim \Sigma/\hbar\omega_D \gg \Sigma/E_F$, where ω_D is the Debye frequency). Therefore to order $\hbar\omega_D/E_F \sim 10^{-2}$ one can neglect the k dependence of Σ and obtain

$$N_T(E) = \sum_k \left|\frac{\Sigma_2(E)/\pi}{[E-\epsilon_k-\Sigma_1(E)]^2+\Sigma_2^2(E)}\right| \approx N(E), \tag{42}$$

where we again assume $N(E)$ varies slowly on the scale of energies of Σ, which for metals is of order $\hbar\omega_D \ll E_F$. Again, we retrieve the simple noninteracting result, despite the fact that the specific heat density of states (i.e., the quasiparticle density of states) is increased by the factor

$$\frac{m^*}{m} = \frac{1 - [\partial\Sigma(\varepsilon, E)/\partial E]}{1 + [\partial\Sigma(\varepsilon, E)/\partial\varepsilon]}\bigg|_{\varepsilon=E=0} \approx 1.5\text{–}2.0 \tag{43}$$

in most metals due to the electron–phonon interaction. Therefore if the tunneling matrix element and band density of states are slowly varying on the scale of $\hbar\omega_D$, phonon structure is expected in the tunneling characteristic only on the scale of $\hbar\omega_D/E_F$.

Weak Coupling Superconductors

We already saw that

$$\begin{aligned} \frac{N_T(E)}{N(0)} &= \frac{|E|}{(E^2 - \Delta^2)^{1/2}}, \qquad E > 0, \\ &= 0, \qquad\qquad E < 0, \end{aligned} \tag{44}$$

where $E > 0$ and < 0 correspond to electron and hole injection, respectively. One has from the pairing theory in the weak coupling limit

$$G(k, E) = \frac{u_k^2}{E - E_k + i\delta} + \frac{v_k^2}{E + E_k - i\delta}. \tag{45}$$

From this expression we find the tunneling density of states is

$$N_T(E) = \sum_k \{u_k^2\, \delta(E - E_k) + v_k^2\, \delta(E + E_k)\}. \tag{46}$$

As in the calculation of the tunneling current, we sum over the twofold degenerate states k_1 and k_2, having $\varepsilon_{k_1} = -\varepsilon_{k_2}$, in pairs so that the u_k^2 and v_k^2 factors each sum to unity. We then have

$$\begin{aligned} \frac{N_T(E)}{N(0)} = \int_0^\infty d\varepsilon_k\, \delta(|E| - \varepsilon_k) &= \left|\frac{d\varepsilon}{dE}\right| = \frac{|E|}{(E^2 - \Delta^2)^{1/2}}, \qquad E > 0, \\ &= 0, \qquad\qquad E < 0, \end{aligned} \tag{47}$$

as required. Notice that if $\Delta = \Delta(k, E)$, one must carefully distinguish the variation with respect to k and to E. As we will see, the strongly retarded nature of the phonon interaction between electrons ensures that in the normal metal Δ, like Σ, varies rapidly with E but slowly with k.

Strong Coupling Superconductors

There are two major shortcomings of the weak coupling theory of superconductivity discussed above. First, the interactions between electrons are assumed to be instantaneous, while we know that the phonons move with a phase velocity which is very small compared to the Fermi velocity, so that a phonon wave packet set up at one point in space by an electron takes a large time to propagate to another point in space where it influences the motion of another electron. Thus we expect retardation effects to play an important role. In addition, the finite lifetime of excited states is neglected in the weak coupling theory, and these damping effects can become important in determining the properties of the superconducting state. Since Hamiltonian dynamics cannot treat potentials which are retarded in time, the problem has been treated by the Green's function scheme. This problem was first studied by Nambu and by Eliashberg.

Here we merely summarize the results of the Green's function treatment. One finds that for a superconductor $G(k, E)$ is given by

$$G(k, E) = \frac{E + \varepsilon(k, E)}{Z(E)[E^2 - \varepsilon^2(k, E) - \Delta^2(E)]}, \tag{48}$$

where $Z(E)$ plays the role of a renormalization function through the relation

$$\varepsilon(k, E) = \varepsilon_k/Z(E). \tag{49}$$

The quantity $\Delta(E)$ is the analog of the energy gap parameter Δ_k of the weak coupling theory. In general, $Z(E)$ and $\Delta(E)$ are complex quantities, and at zero temperature they satisfy the coupled integral equations (the analog of the energy gap equation of the weak coupling theory),

$$\Delta(E) = \frac{1}{Z(E)} \int_0^{\hbar\omega_c} \mathrm{Re}\left\{\frac{\Delta(E')}{[E'^2 - \Delta^2(E')]^{1/2}}\right\} [K_+(E, E') - K_c]\, dE', \tag{50a}$$

$$[Z(E) - 1]E = \int_0^\infty \mathrm{Re}\left\{\frac{E'}{[E'^2 - \Delta^2(E')]^{1/2}}\right\} K_-(E, E')\, dE'. \tag{50b}$$

The interaction kernels are given by

$$K_\pm(E, E') = N(0) \int \alpha^2(\nu) g(\nu) \left\{\frac{1}{E' + E + \nu - i\delta} \pm \frac{1}{E' - E + \nu - i\delta}\right\} d\nu, \tag{51}$$

where $\alpha^2(\nu)g(\nu)$ is the product of the square of the electron–phonon matrix element and the phonon density of states averaged over all phonon modes

of energy ν. The kernel K_c is the Coulomb pseudopotential. For a model in which the screened Coulomb matrix element times the density of electron states is taken to be a constant, $N(0)V_c$, in a band of width $2\hbar\omega_m$ centered at the Fermi surface and zero outside this band one has

$$K_c = \frac{N(0)V_c}{1 + N(0)V_c \log(\omega_m/\omega_c)}, \tag{52}$$

where ω_c is a cutoff which may be chosen for computational convenience, so long as $\omega_D \ll \omega_c < \omega_m$.

Numerical solutions of (50*a*), (50*b*), and (51) have been obtained for a variety of assumed forms for $\alpha^2(\nu)g(\nu)$. For Pb one knows from neutron inelastic scattering that $g(\nu)$ has peaks near 4 and 8.5 meV, corresponding to transverse and longitudinal phonons, respectively. Scalapino *et al.*, in an attempt to explain the tunneling results of Rowell and co-workers on superconducting Pb, assumed a simple two-Lorentzian form for $\alpha^2(\nu)g(\nu)$ and obtained the results shown in Figs. 5(*a*) and 5(*b*). By combining (35) with (48) one finds the tunneling density of states is given by the remarkably simple expression

$$N_T(E) = \mathrm{Re}\{|E|/[E^2 - \Delta^2(E)]^{1/2}\}. \tag{53}$$

By combining the solutions shown in Figs. 5(*a*) and 5(*b*) with this relation one obtains the results shown in Fig. 5(*c*). The experimental results are shown for comparison, and one sees a remarkable agreement between theory and experiment even for this oversimplified model of $\alpha^2(\nu)g(\nu)$. More recently McMillan has inverted Eqs. (50*a*), (50*b*), (51), and (53) to determine $\alpha^2(\nu)g(\nu)$ and K_c directly from the tunneling characteristic. In general, the results are in reasonably good agreement with those of neutron inelastic scattering.

The above treatment can be readily extended to finite temperature, although the general features of the results, i.e., wiggles of dI/dV for V of order Δ plus the energy of a peak of $\alpha^2(\nu)g(\nu)$, persist. For Pb, a strong coupling superconductor, the phonon anomalies occur on a scale of a few per cent, while the effects are smaller for weaker coupling materials.

CONCLUSION

While the theory of single-particle tunneling in superconductors can be handled in a quantitative manner regardless of the electron–phonon coupling strength, there remains the problem of excitations on or near the

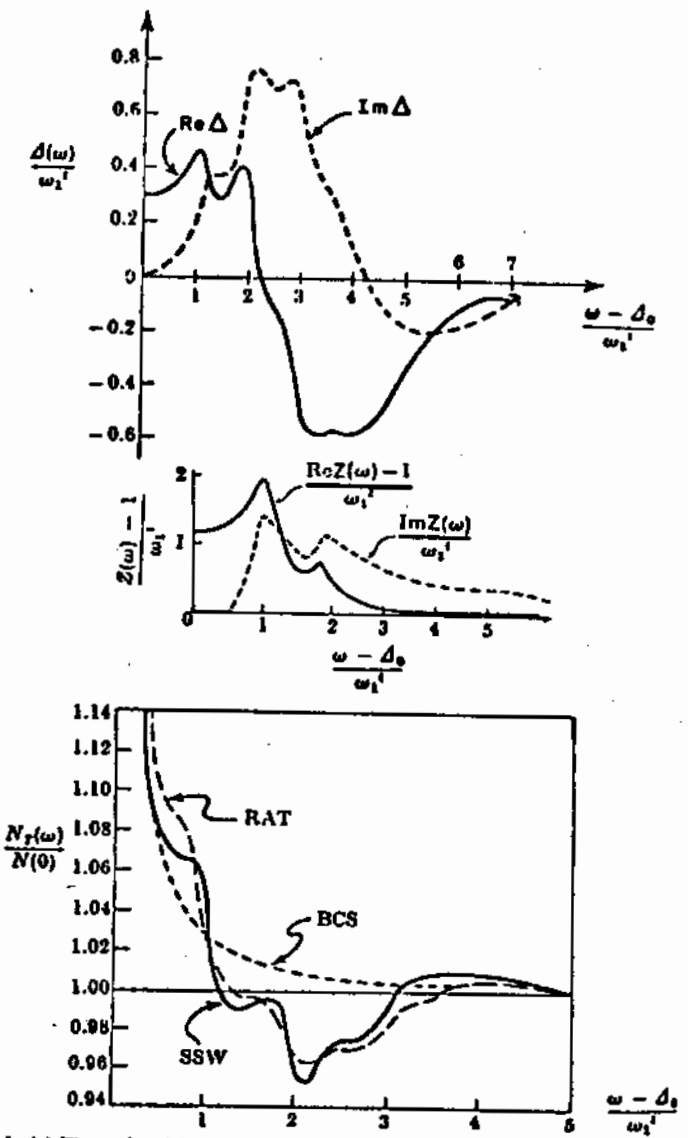

Fig. 5. (*a*) The real and imaginary parts of the gap function plotted as a function of energy for the case of a simple model of lead. (*b*) Comparison of the tunneling density of states predicted theoretically on the basis of the gap shown in (*a*) with the experimental results of Rowel *et al.* on lead.

interface leading to additional structure, as first discussed by Lambe and Jaklevic. There is also the question of whether $\alpha^2(\nu)g(\nu)$ for phonons in the vicinity of the interface, where the tunneling process takes place, is appreciably distorted from the bulk value of this function. The close agreement with the neutron results suggest the distortion is not large. Nevertheless, a finite value of $\alpha^2(\nu)g(\nu)$ is deduced from the tunneling data on many materials for ν greater than the upper cutoff of the bulk phonon spectrum. A detailed understanding of this surface-bulk interplay must await further work. It is clear, however, that single-particle tunneling in superconductors is a very rich phenomenon for gaining insight into the structure of the superconducting state as well as for providing a powerful tool for investigating parameters important in the normal-state properties of the material [e.g., $\alpha^2(\nu)g(\nu)$] and interface excitations.

REFERENCES

An extensive list of references related to the above discussion is contained in J. R. Schrieffer, Theory of Superconductivity, W. A. Benjamin, Inc., New York, 1964, pp. 78–87, 188–193. A more recent review of tunneling in superconductors is given by W. L. McMillan and J. M. Rowell in: Treatise on Superconductivity (R. D. Parks, ed.), Marcel Dekker, New York, 1968.